Planta (2019) 250:1867–1879
https://doi.org/10.1007/s00425-019-03269-1

ORIGINAL ARTICLE

Cellulose-rich secondary walls in wave-swept red macroalgae fortify flexible tissues

Patrick T. Martone[1,2] · Kyra Janot[1,2] · Miki Fujita[2] · Geoffrey Wasteneys[2] · Katia Ruel[3] · Jean-Paul Joseleau[3] · José M. Estevez[4,5]

Received: 4 March 2019 / Accepted: 27 August 2019 / Published online: 3 September 2019

Abstract

Main conclusion **Cellulosic secondary walls evolved convergently in coralline red macroalgae, reinforcing tissues against wave-induced breakage, despite differences in cellulose abundance, microfibril orientation, and wall structure.**

Abstract Cellulose-enriched secondary cell walls are the hallmark of woody vascular plants, which develop thickened walls to support upright growth and resist toppling in terrestrial environments. Here we investigate the striking presence and convergent evolution of cellulosic secondary walls in coralline red algae, which reinforce thalli against forces applied by crashing waves. Despite ostensible similarities to secondary wall synthesis in land plants, we note several structural and mechanical differences. In coralline red algae, secondary walls contain three-times more cellulose (~ 22% w/w) than primary walls (~ 8% w/w), and their presence nearly doubles the total thickness of cell walls (~ 1.2 µm thick). Field emission scanning electron microscopy revealed that cellulose bundles are cylindrical and lack any predominant orientation in both primary and secondary walls. His-tagged recombinant carbohydrate-binding module differentiated crystalline and amorphous cellulose in planta, noting elevated levels of crystalline cellulose in secondary walls. With the addition of secondary cell walls, *Calliarthron* genicular tissues become significantly stronger and tougher, yet remain remarkably extensible, more than doubling in length before breaking under tension. Thus, the development of secondary walls contributes to the strong-yet-flexible genicular tissues that enable coralline red algae to survive along wave-battered coastlines throughout the NE Pacific. This study provides an important evolutionary perspective on the development and biomechanical significance of secondary cell walls in a non-model, non-vascular plant.

Keywords Biomechanics · Carbohydrate-binding module · *Calliarthron* · Convergent evolution · Coralline · Genicula · Intertidal · Macroalgae · Rhodophyta · Seaweed

✉ Patrick T. Martone
pmartone@mail.ubc.ca

Kyra Janot
kjanot@gmail.com

Miki Fujita
mikifj@mail.ubc.ca

Geoffrey Wasteneys
geoffrey.wasteneys@ubc.ca

Katia Ruel
katiaruel@yahoo.fr

Jean-Paul Joseleau
jpjoseleau@gmail.com

José M. Estevez
jestevez@leloir.org.ar

[1] Biodiversity Research Centre, University of British Columbia, Vancouver, BC V6T 1Z4, Canada

[2] Botany Department, University of British Columbia, Vancouver, BC V6T 1Z4, Canada

[3] E.I. LINK-Conseil, 349 rue du Mont-Blanc, 38570 Le Cheylas, France

[4] Fundación Instituto Leloir and Instituto de Investigaciones Bioquímicas Buenos Aires, Consejo Nacional de Investigaciones Científicas y Técnicas (IIBBA-CONICET), C1405BWE Buenos Aires, Argentina

[5] Centro de Biotecnología Vegetal, Facultad de Ciencias Biológicas, Universidad Andres Bello, Santiago, Chile

Abbreviations

CBM	Carbohydrate-binding module
CW	Cell wall
FESEM	Field emission scanning electron microscopy
TC	Terminal complex

Introduction

Cell walls play critical roles in the development, growth, structure, and mechanics of plants, and the performance of cell walls depends directly upon the chemical composition, orientation, and interactions among constitutive macromolecules, especially cellulose (Kloareg and Quatrano 1988; Plomion et al. 2001; Niklas 2004; Somerville 2006; Nishiyama 2009; Cosgrove and Jarvis 2012; Salmén 2015). For example, simple mutations in cellulose synthesis genes can have profound effects on emergent properties of plants, including growth, morphology, and mechanical properties (Turner and Somerville 1997; Arioli et al. 1998; Somerville et al. 2004; Yamaguchi et al. 2011; Li et al. 2014; Chantreau et al. 2015). Thus, researchers have long studied the biochemistry and molecular structure of cellulosic walls to better understand myriad functional aspects of plants.

In general terms, most plants lay down two distinctive cell walls: primary walls, which are deposited by actively growing cells and are thin and extensible under cellular turgor pressure (Evert 2006; Geitmann 2010), and secondary walls, which are deposited after cells have stopped growing and are much thicker and more rigid than primary walls, and completely resistant to cellular turgor pressure (Salmén and Burgert 2009). Cellulose microfibrils within primary walls often form a dynamic network that may be disordered or aligned to direct expansion of growing cells depending on cell types (Fujita and Wasteneys 2014). In contrast, cellulose microfibrils within secondary walls typically comprise highly ordered networks fortified with lignin that provide robust biomechanical support to stems, permitting hydraulic transport and upright growth in air (Cosgrove and Jarvis 2012).

Our understanding of the important chemical, structural, and biomechanical differences between primary and secondary walls is based almost exclusively on studies of terrestrial plants (Morrison et al. 1993; Harris 2006; Gierlinger 2014; Joseleau and Perez 2016), albeit with insight from unicellular algae (e.g., Giddings et al. 1980; Kim et al. 1996; Rydahl et al. 2015), so conclusions about the adaptive significance and evolution of secondary walls have been largely confined to the development of vascular tissue and growth on land. Contrary to this paradigm was the discovery of secondary walls in the wave-swept red macroalga *Calliarthron cheilosporioides* (Martone et al. 2009) and other closely related corallinoid macroalgae (Janot and Martone 2016). Because red and green algae diverged from a common single-celled ancestor more than 1 billion years ago (Yoon et al. 2004), secondary walls produced by macrophytes within the two groups represent convergent evolution (Martone et al. 2009). The degree of convergence is striking: during xylem development, fiber cells elongate, thicken their walls, and lose cytoplasm and organelles (Mutwil et al. 2008), and in corallinoid genicula (flexible support tissues), cells elongate (approximately tenfold in *Calliarthron* (Martone 2007a), partially lose cytoplasm and organelles, and cell wall thickness doubles (Johansen 1981; Martone 2007a; Janot and Martone 2016). Moreover, their cell walls contain lignin (Martone et al. 2009) and stain positively for cellulose (Martone 2007b). Fully mature genicular cells bear close visual resemblance to xylem fibers (Martone et al. 2009). As in xylem fibers, genicular cells with thickened walls function in mechanical support, specifically reinforcing corallinoid genicular tissues against forces imposed by crashing waves (Martone 2006, 2007a; Martone and Denny 2008; Janot and Martone 2016). The presence of secondary walls in a marine alga challenges our understanding about the role of these structures in macrophytes, since marine macroalgae lack hydraulic transport, are mostly isotonic with their surroundings with less need to resist turgor, and primarily need to resist drag, rather than gravity, to stay upright. Thus, these distinctive wave-swept seaweeds provide a new perspective and unique opportunity to test our basic assumptions about cellulose content, microfibril orientation, and biomechanical impact of secondary walls.

Cellulose content

The chemical composition of cell walls in *Calliarthron* and other corallinoid macroalgae has been well characterized and includes primarily sulphated galactans, glycoproteins, and cellulose (Cases et al. 1994; Takano et al. 1996; Usov and Bilan 1996; Usov et al. 1997; Bilan and Usov 2001; Navarro and Stortz 2002; Martone et al. 2010). Because walls of corallinoid macroalgae have not been reported to contain hemicelluloses, such as xylans or mannans found exclusively in other red algae (Matulewicz et al. 1992; Kolender et al. 1995; Stortz and Cerezo 2000), the quantification of water-insoluble glucose units in corallinoid tissue should be indicative of cellulose.

Primary walls in land plants, such as *Arabidopsis*, contain 10–20% cellulose, and secondary walls contain double that amount, up to 40% cellulose (Carroll et al. 2012). By comparison, red algal cell walls generally contain 1–8% (rarely up to 20%) cellulose (w/w; Kloareg and Quatrano 1988). Further, some red algae are known to produce lamellate walls (Myers and Preston 1959; Kloareg and Quatrano 1988; Tsekos et al. 1993). However, the structure of cell wall

layers appears to be similar and the chemical composition is presumed to be the same. If secondary walls in corallinoid genicula are added for mechanical support, as in land plants, then we hypothesize that the cellulose content of secondary walls will be significantly higher than that of typical primary walls.

Microfibril orientation

Cellulose microfibrils are generally produced at the plasma membrane by terminal complexes (TC) of particles composed of cellulose synthases (CesA's) (Saxena and Brown 2005; Sethaphong et al. 2013), and the structure of cellulose microfibrils across algal taxa generally varies with TC geometry (Delmer 1991; Tsekos 1999). In land plants, terminal complexes are composed of rosettes, whereas in bacteria, brown algae, and red algae, terminal complexes are linear with particles arranged in 1–4 rows (see Tsekos 1999). Rosette TCs in land plants universally produce microfibrils that are cylindrical, with a diameter of 2–3 nm (Thomas et al. 2013; Li et al. 2014), whereas most organisms with linear TCs produce flat ribbon-like microfibrils (Tsekos et al. 1993; Tsekos 1999). Florideophyte red algae are a major exception with linear TCs producing microfibrils that are largely cylindrical and have diameters of 4–5 nm, similar to those produced by rosette TCs in land plants (Tsekos et al. 1993; Tsekos 1999). How linear TCs in Florideophyte red algae uniquely produce cylindrical microfibrils is unknown. In plant primary walls, cellulose microfibrils are often disordered, but during rapid expansion they can be uniformly aligned to constrain cell expansion in one direction (Cosgrove 2005; Geitmann 2010), while microfibrils in some secondary walls are normally highly ordered to resist cell deformation (Plomion et al. 2001; Emons et al. 2002; Cosgrove 2005; Salmén and Burgert 2009). In contrast, cellulose microfibrils in red algal cell walls are often disordered (Tsekos et al. 1993) even during cell expansion (Waaland and Waaland 1975), although parallel-oriented microfibrils have also been documented in a few species (Tsekos et al. 1993). We hypothesize that corallinoid genicular primary walls contain disordered microfibrils as occurs in walls produced by other red algae, but that secondary walls would have highly ordered microfibrils similar to land plants.

Biomechanical properties

The great abundance of cellulose and the highly ordered nature of microfibrils within secondary walls underlie the high strength (i.e., breaking stress; break force per area), high stiffness (i.e., modulus; force to stretch per area), and low extensibility (i.e., breaking strain; extension to break) of land plants (Burgert 2006), whereas the lower abundance of cellulose and disordered nature of microfibrils in red algae likely underlie the lower strength, lower stiffness, and greater extensibility of most red macroalgae (Hale 2001). However, mechanical properties of genicula in coralline species are different: stronger, stiffer, and yet more extensible under stress than other algal tissues and thus somewhat intermediate between macroalgae and land plants (Martone 2006, 2007a; Denny et al. 2013; Janot and Martone 2016). Genicular strength, in particular, positively correlates with cellulose content across coralline species (Janot 2018). We hypothesize that the production of cellulosic secondary walls plays an important role in augmenting the biomechanical properties of these distinctive red algae.

In this study, we investigate the abundance, structure, orientation, and biomechanical impact of cellulose within primary and secondary walls of two coralline species: *Calliarthron tuberculosum* and *C. cheilosporioides.* These two species are very closely related (Gabrielson et al. 2011), and they are chemically, morphologically, biomechanically, and ecologically similar (Martone 2006, 2007a; Janot and Martone 2016). We quantify the abundance of cellulose produced by *C. cheilosporioides* using analytical chemistry to see if the abundance of cellulose in secondary walls is greater than that produced in primary walls. We use His-tagged carbohydrate binding modules (CBMs) (Blake et al. 2006; Ruel et al. 2012; Voiniciuc et al. 2018) to localize and differentiate crystalline and amorphous cellulose within the walls of *C. tuberculosum*, and quantify the relative abundance of these microstructures in primary and secondary walls. We also visualize cellulose microfibrils in planta using field emission scanning electron microscopy (FESEM) to see if microfibril orientation differs between primary and secondary walls. Ultimately, we test the hypothesis that the development of cellulosic secondary walls augments the biomechanical properties of *C. cheilosporioides,* as in land plants, contributing to the mechanical support and survival of fronds in the hydrodynamically stressful intertidal zone.

Materials and methods

Sample collection

Specimens of *C. cheilosporioides* Manza, both young sprouts (3–5 cm tall) and old fronds (12–20 cm tall), were collected from the wave-swept intertidal zone of Hopkins Marine Station, Pacific Grove, CA (36 37′18.5″N, 121 54′20.1″W) and analyzed for polysaccharide content and biomechanical properties. Specimens of *C. tuberculosum* (Postels & Ruprecht) E.Y. Dawson, all old fronds (12–15 cm tall), were collected from intertidal tidepools at Botanical Beach, Vancouver Island, BC, Canada (48 31′48″N, 124

27′18″W) and used for CBM cellulose localization and FESEM imaging.

Isolation of water-soluble and water-insoluble cell wall fractions

In order to compare the chemical composition of primary walls and secondary walls in *C. cheilosporioides*, we analyzed cell walls from young sprouts (primary walls only) and cell walls from old fronds (primary and secondary walls) (see Martone 2006, 2007a). The cell wall (CW) fraction isolation procedures were similar to those described elsewhere (Cases et al. 1994; Navarro and Stortz 2002) with minor modifications. Genicular segments were separated from the intergenicular regions and both were analyzed separately in the same way as the whole plants. Briefly, ball-milled whole plants (15 g) and intergenicula (3 g) from young and old individuals of *C. cheilosporioides* were each suspended in water (20 ml/g), respectively, and diluted HCl was added drop-wise (not allowing the pH to drop below 6) with mechanical stirring until no more CO_2 evolution was detected. The solution obtained after stirring for 24 h at room temperature (RT) and 6 h at 90°C was cooled down, neutralized, incubated with α-amylase (Sigma) for 24 h at RT to degrade the floridean starch, dialyzed (molecular weight cut off 6.0–8.0 kDa), and freeze-dried. The product obtained was the water-soluble cell wall fraction (water-soluble CW) enriched in xylogalactans (i.e., agarans). The remaining water-insoluble cell wall material (water-insoluble CW) rich in cellulose was freeze-dried as a separate fraction. Isolated genicula from young and old individuals (15 and 20 mg, respectively) were also ball-milled and extracted as described, but without the addition of HCl during the initial water extraction.

Monosaccharide composition

Total sugar content was analyzed by phenol–sulfuric acid method (Dubois et al. 1956) without previous hydrolysis of the polysaccharide. To determine the monosaccharide composition of water-soluble CW fraction, alditol acetates were obtained by reductive hydrolysis and acetylation of the samples (Stevenson and Furneaux 1991). Briefly, reductive hydrolysis of the water-soluble CW fractions (1–3 mg) were carried out at 80 °C in a solution of 0.4 ml TFA 3 M with the addition of 0.1 ml of 4-metilmorfoline borane (MMB) (80 mg/ml) for 10 min. Then, 0.1 ml of the same MMB solution was added and the vial for heated to 120 °C for 2 h. Finally, 0.2 ml of MMB solution was added and the sample was dried out to eliminate the excess of TFA. Then, the mixture of hydrolyzed sugars was acetylated with anhydride acetic acid (0.2 ml) and concentrated TFA (0.2 ml) in an oven at 60 °C for 10 min. The solution was cooled down and then extracted in 1 ml chloroform/water (1:1) keeping the chloroform phase, which was washed with 0.5 ml sodium bicarbonate (three times) and H_2O (twice). Finally, the remaining water was extracted with sodium sulfate anhydrous and the chloroform extract was dried under nitrogen. Alditol acetates were analyzed by gas liquid chromatography coupled to mass spectrometry (GLC–MS) (Stevenson and Furneaux 1991). GLC–MS analysis of the alditol acetates was carried out on a Hewlett–Packard 5890A gas–liquid chromatography equipped with a flame ionization detector and fitted with a fused-silica column (0.25 mm i.d. × 30 m) WCOT-coated with a 0.20-mm film of SP-2330. Chromatography was programmed from 200 (5 min hold) to 230 °C at 2 °C/min.

To analyze the water-insoluble CW fraction that contains mostly cellulose, 1–3 mg of it was dissolved in 100% TFA (37 °C, 1 h), followed by dilution of the acid to 80%, heating at 100 °C for 1 h, and further dilution to 2 M (Morrison 1988). Hydrolysate was derivatized to the corresponding alditol acetates and analyzed by GLC–MS as indicated before. In both types of hydrolysis (strong hydrolysis for water-insoluble CW fraction and reductive hydrolysis for the water-soluble CW fractions), inositol was as internal standard. Total (xylo)galactan sulfate content was estimated from four replicates of water-soluble CW fractions obtained from genicula, intergenicula, and whole plants (see polysaccharide extraction). It was calculated based on the sulfate content estimated by the method of Dodgson and Price (1962) plus total galactose (including all mono-methylated galactoses) and xylose contents obtained from alditol acetates (by the reductive hydrolysis method). We discounted other minor monosaccharides obtained such as glucose, mannose, and arabinose that are not part of the xylogalactan structure, deriving from starch and traces of other glycans, respectively (see Table 1). Total cellulose content was estimated using three replicates of water-insoluble CW fractions subjected to a strong hydrolysis as described above (see Morrison 1988). The calculation of cellulose content was made based on glucose units.

Field emission scanning electron microscopy (FESEM)

Samples of *C. tuberculosum* were prepared for FESEM using a technique developed for analysis of cellulose microfibrils in *Arabidopsis* (Sugimoto et al. 2000; Marga et al. 2005; Fujita and Wasteneys 2014) and Characean internodal cells (Foissner and Wasteneys 2012, 2014). Segments of *C. tuberculosum* were excised with a razor blade into 5 mm lengths, fixed in 1% (v/v) glutaraldehyde and 4% formaldehyde made up in PME buffer (25 mM PIPES, 0.5 mM MgSO4, and 2.5 mM EGTA, pH 7.2) for 6 h, rinsed three times for 10 min in PME buffer, and decalcified in 1 M HCl

Table 1 Carbohydrate analyses of water-soluble CW fraction and water-insoluble CW fraction isolated from whole plants, genicula, and intergenicula of *Calliarthron cheilosporioides*

Sample and cell types[a]	Cellulose[b] ($n=3$), %	(Xylo)galactan[c] ($n=3$), %	Type of hydrolysis[d]	Average monosaccharide composition (mol%)[e,f] ($n=3$)					
				Glc	Gal	2-Gal	6-Gal	Xyl	Man
Whole plants									
Young	–	5.6 (±0.8)	A	tr.[g]	62.4	9.2	8.2	17.1	3.1
Old	–	6.4 (±0.6)	A	3.3[g]	49.1	12.2	7.6	16.4	11.4
Young	17.0 (±2.0)	5.3 (±0.8)[g]	B	76.8[h]	15.0	2.5	1.6	2.6	1.5
Old	14.0 (±2.5)	7.5 (±1.5)[g]	B	64.1[h]	25.2	2.7	2.5	3.0	2.5
Genicula									
Young	–	11.1 (±0.8)	A	tr.[g]	78.0	2.4	14.6	2.9	2.1
Old	–	13.4 (±1.2)	A	tr.[g]	72.5	2.4	19.4	2.9	2.8
Young	8.0 (±1.3)	11.5 (±1.4)[g]	B	41.9[h]	48.9	tr.	9.2	tr.	tr.
Old	15.0 (±1.5)	14.2 (±1.1)[g]	B	52.3[h]	38.3	tr.	9.4	tr.	tr.
Intergenicula									
Young	–	5.0 (±0.9)	A	tr.[g]	55.1	8.3	7.1	24.5	5.0
Old	–	6.0 (±1.0)	A	tr.[g]	55.8	11.3	7.1	20.7	5.1
Young	14.0 (±2.0)	5.0 (±0.9)[g]	B	74.0[h]	14.8	3.4	1.6	3.9	2.3
Old	14.0 (±1.8)	6.5 (±0.8)[g]	B	66.3[h]	22.1	3.4	2.9	3.4	1.9

Young (3–5 cm tall) and old (12–15 cm) plants were analyzed separately for comparison. Water-soluble CW fractions are primarily composed of xylogalactans and water-insoluble CW fractions are primarily composed of cellulose with minor traces of xylogalactans

[a]Initial material after decalcification, α-amylase treatment, and dialysis (see "Materials and methods")

[b]Based on the glucose content on the TCW measured by acid hydrolysis method for insoluble materials (Morrison 1988). Inositol was used as internal standard in both types of hydrolysis

[c]Total amounts of water-soluble (xylo)galactans in the original sample were quantified by the reductive hydrolysis method (Stevenson and Furneaux 1991). An average of 5.8% (w/w) of sulfate (as SO_3Na) was detected for genicula segments and 4.7% (w/w) of sulfate (as SO_3Na) for intergenicula cell walls (Martone et al. 2010)

[d]TCW were analyzed by two different methods of hydrolysis: (A) reductive hydrolysis (Stevenson and Furneaux 1991) for soluble polysaccharides, and (B) acid hydrolysis for insoluble materials (Morrison 1988)

[e]Small amounts of arabinose were detected in most of the fractions

[f]2-Gal = 2-*O*-methyl galactose

[g]Glucose derived from starch

[h]Glucose derived from cellulose

for 20 min. Samples were cryoprotected in 25% and 50% (v/v) DMSO in PME buffer for 10 min each, then placed on a pinhead with tissue-tek embedding media (Tissue-tek OCT compound, Sakura) and frozen in liquid nitrogen. The samples were then cryo-planed with a glass knife in a cryo-chamber maintained at − 130 °C. The surface of the tissue was sliced off with a glass knife set at a 6° angle with a speed of 0.6 mm/s on a cryo-ultra-microtome (Ultracut T ultramicrotome with Leica EM FCS attachment, Leica). The remaining portion of the tissue on the pinhead was thawed in 50% (v/v) DMSO in PME buffer and rinsed in PME buffer. To extract cytoplasmic materials, cryo-planed samples were incubated either in 0.5% or 1.0% sodium hypochlorite solution for 10 min on a rotary shaker followed by three 10 min washes in distilled water. The samples were further incubated with 2% OsO_4 for 1 h at room temperature and washed in distilled water three times for 10 min. After dehydration with an ethanol series (30, 50, 70, 95, and 100% three times, 2 h each step), samples were critical point dried in an Autosamdri 815B critical point dryer (Tousimis) using CO_2 with a purge time of 15 min. The cut surfaces of the samples were placed upward, mounted on aluminum stubs with double-sided sticky carbon tape, and then coated with Pt/Pd (80/20) at 40 mA to a 5-nm thickness (High resolution sputter coater 208HR, Cressington). Cellulose microfibrils were observed with a Hitachi S4700 SEM set at 3 kV and 10 µA current. High-resolution images were taken with an upper detector and with a working distance between 5 and 6 mm. Objective and beam apertures were set at 3 and 2, respectively.

Cellulose binding domain (CBM) localization

In order to examine the distribution of cellulose within *Calliarthron* genicula, we decalcified, resin-embedded, and thin-sectioned thalli, and probed cell walls directly

in planta with two recombinant His-tagged carbohydrate-binding modules (CBMs) specific to crystalline cellulose (CBM3a) and amorphous cellulose (CBM28) (McLean et al. 2002; Blake et al. 2006), respectively. CBM3a and CBM28 have been used to successfully differentiate several classes of crystalline, para-crystalline, and amorphous microstructures of cellulose in plant cell walls (Blake et al. 2006; Ruel et al. 2012). The specificity of these two binding modules is due to the respective topology of their binding sites, CBM3a interacting with the flat surface of crystalline cellulose, and CBM28 interacting with free single chains of amorphous cellulose by the cleft displayed in its binding site (Lehtiö et al. 2003).

Segments of *C. tuberculosum* were fixed overnight in 5% formalin seawater. Fixed specimens were decalcified overnight in 1 M HCl, then dehydrated in increasing concentrations of ethanol (25%, 50%, 75%, and 100%) for 1 h per treatment. Specimens were left in 100% ethanol overnight, then placed in medium-grade LR White embedding resin overnight. Specimens were placed in gel capsules, immersed in fresh LR White, and baked at 62 °C for 1.5 h.

CBMs were His-tagged recombinant CBM3a from *Clostridium thermocellum* and CBM28 from *Bacillus* sp. 1139, expressed in *Escherichia coli* as described in Blake et al. (2006). The freeze-dried CBM3a (directed to crystalline cellulose) and CBM28 (directed to non-crystalline regions of cellulose) were reconstituted in distilled water to give "mother solutions" at concentrations of 100 µg/ml and 10 µg/ml for CBM3a and CBM28, respectively. Ultrathin sections (50 nm thick) were cut with a Leica EM UCG ultramicrotome (Leica Micro Systems) using a diamond knife, collected on plastic rings as described earlier, and labeled in three steps as described in Ruel et al. (2012). Briefly, ultrathin sections were first blocked for non-specific labeling with PBS containing 5% non-fat dry milk (w/v) (30 min), then incubated on a series of dilutions of CBMs in PBS/5% milk to determine the optimal dilution of CBMs to be used. Optimal dilutions retained for CBM3a and CBM28 were 0.25 µg/ml and 0.625 µg/ml, respectively. Incubation time with the CBMs was 1.5 h at room temperature. After rinsing with PBS, sections were incubated with an unconjugated polyclonal His-Tag (Rabbit) antibody (MBL, Biovalley, Marne-La-Vallée, France) diluted 1/100 (v/v) in PBS/5% milk for 1 h at RT and then overnight at 4 °C. After rinsing with PBS, sections were then incubated on protein A-gold commercial complex (PAG5, TEBU) diluted 1/30 in PBS/fish gelatin 0.15% (w/v) for 1.5 h. After careful rinsing in PBS, sections were fixed in 2% glutaraldehyde in water and then thoroughly rinsed in water to eliminate possible salt presence before silver enhancing with SPI-Mark™ silver enhancement kit (SPI Supplies). Sections were finally collected on carbon-coated grids and contrasted with uranyl acetate (2 min). Omission of the CBM-binding step or the unconjugated anti-His antibody step gave no labeling thus eliminating a false positive due to secondary markers. Immunolabeling experiments were repeated 2–3 times on independent blocks of algal material, and all observations were carried out on approximately 15 sections per grid. Photographs were taken with a Philips CM200-T cryo-electron microscope at an accelerating voltage of 80 kV, with Kodak 4489 films, and 60–80 images were investigated per grid. The negatives were scanned (EPSON Perfection 4990 PHOTO Scan) in.tif quality at 300 dpi resolution.

All comparative immunolabeling experiments were carried out in parallel in order to keep the same experimental conditions. For quantitative estimation of the labeling, several sections of the alga were used for each CBM. The number of gold particles per 1 μm^2 was counted manually and relative labeling indices were calculated. Because each CBM has its own substrate affinity, one cannot directly compare the absolute response (number of gold particles) for each CBM. Thus, we assigned a value of 1.0 to the S1 sub-layer to serve as a reference for each CBM, respectively (Ruel et al. 2001; Mayhew et al. 2004).

Biomechanical properties

Pull-to-break tests were performed on *C. cheilosporioides* fronds ($n = 25$) as described in Martone (2006). To quantify the properties of old genicula (with both primary and secondary walls), segments near the bases of large fronds (approx. 20 cm tall) were tested; to quantify the properties of young genicula (with only primary walls), segments near the tips of those same fronds were tested (see Martone 2007a for cell wall differences). Briefly, fronds were held between two sets of aluminum, rubber-lined clamps that moved along a tensometer track. Force was quantified as the deflection of a stationary clamp mounted to two steel beams, measured by a linearly variable differential transformer (LVDT; model 100HR, Schaevitz Engineering, Pennsauken, NJ, USA). Strain was measured directly using a video camera (model TMC-S14, Pulnix Sensors, Sunnyvale, CA, USA) and video dimension analyser (model V94, Living Systems Instrumentation, Burlington, VT, USA), which tracked the relative position of intergenicula flanking individual joints in each stretched specimen. Specimens were pulled at a rate of 60 mm/min until failure. Biomechanical properties of young and old genicula were statistically compared using paired *t* tests (JMP version 10, SAS, Cary, NC).

Results

The fine chemical changes between genicular and intergenicular cell walls in the structure of water-soluble xylogalactans (i.e., agarans) have been previously investigated (Martone

et al. 2010). Based on this, we asked if cell-wall composition also changes throughout the development of primary and secondary cell walls. Targeted water-soluble and water-insoluble polysaccharide extractions of young and old *Calliarthron* thalli (Fig. 1a) allowed us to analyze cell wall chemistry of genicula (Fig. 1b; Table 1) at different stages of maturation—that is, with and without secondary cell walls. A two-step extraction protocol was used to isolate: (1) the water-soluble polysaccharides (mostly xylogalactans), and (2) a water-insoluble fraction (mostly cellulose) (Table 1). Genicular primary walls were composed of approximately 8% (w/w) cellulose and 11% (w/w) water-soluble xylogalactans. The addition of secondary walls nearly doubled the total cellulose content up to 15%, while the levels of xylogalactans remained almost the same (around 13%) (Fig. 1c; Table 1). Calcified intergenicular cell walls isolated from young and old plants contained approximately 2.1% cellulose, which actually represented 14% (w/w) when calculated as a fraction of decalcified dry weight (Fig. 1c) and 5–6% (w/w) xylogalactans. Total cell walls (TCWs, including water-soluble and water-insoluble CW fractions) in genicula increased from approximately 19% dry weight in primary walls to 28% with the addition of secondary walls, while intergenicular TCWs remained the same (19–20%) over development (Fig. 1c; Table 1). Linkage analysis carried out on the water-insoluble CW fractions obtained from genicula and intergenicula showed ~ 50 and ~ 70 mol% of four-linked glucose units, respectively (results not shown).

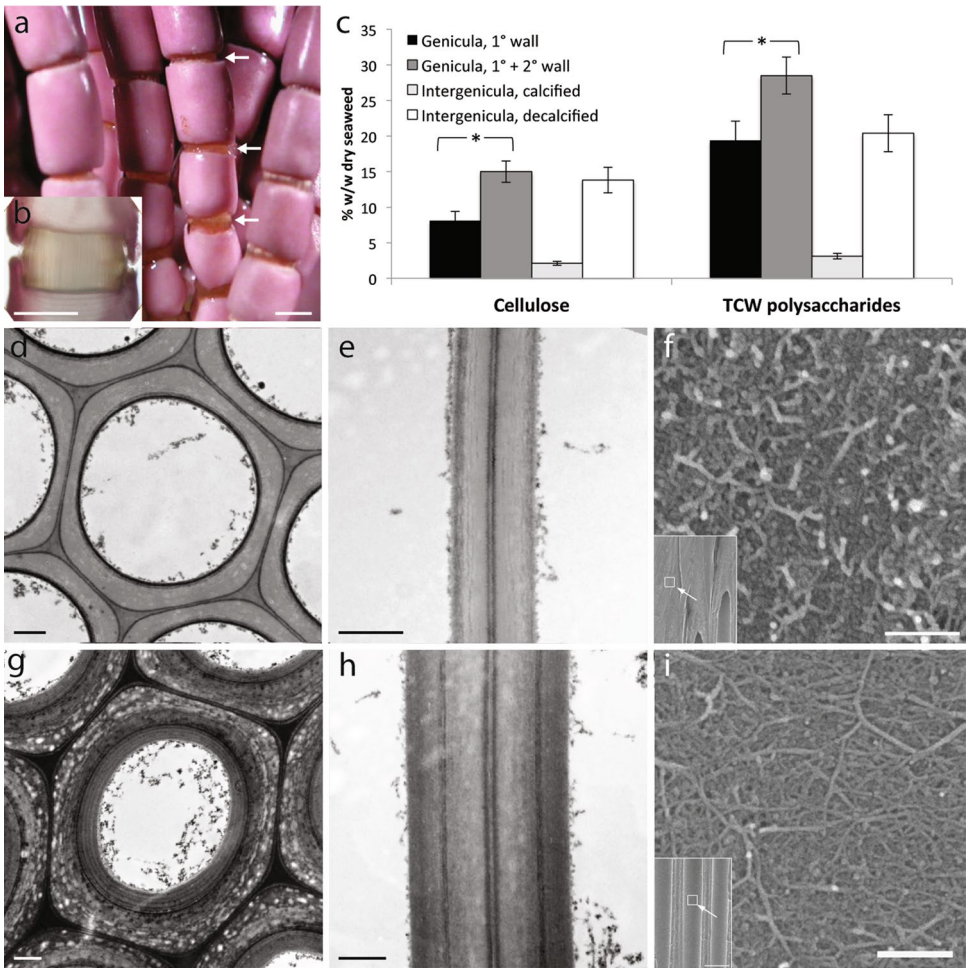

Fig. 1 Summary of thallus and genicular morphology, cellulose quantification, cell wall (CW) structure, and microfibril orientation. **a** *Calliarthron* thalli consist of calcified segments separated by uncalcified joints, called genicula (white arrows). **b** Genicula are composed of a single tier of cells, connecting adjacent segments. **c** Cellulose-enriched water-insoluble CW fraction and total CW fractions (water-soluble CW fraction + water insoluble CW fraction) content increases as genicula age and secondary walls develop. **d** Cross-section and **e** long-section of young geniculum showing primary wall. **f** Cellulose microfibrils in primary wall, imaged from outer surface, have no predominant orientation. **g** Cross-section and **h** long-section of old geniculum showing both primary and secondary walls. **i** Cellulose microfibrils in secondary wall, imaged from inner surface, have no predominant orientation. Insets **f**, **i** cryo-planed longitudinal section of genicular cells with arrows and boxes indicating locations where high-resolution images were taken. Scale bars 1 mm (**a**, **b**), 1 µm (**d**, **e**, **g**, **h**), 200 nm (**f**, **i**), 5 µm (**f**, **i** insets)

The remaining dry weight content of cell walls was not quantified but may be other macromolecules, including proteins, glycoproteins, lipids, sulphates from the xylogalactans, and calcium and sodium ash (Heaney-Kieras et al. 1977; Kloareg and Quatrano 1988; Martone et al. 2010).

Transmission electron micrographs indicated that primary and secondary cell walls in *Calliarthron* were similar in thickness (0.6 ± 0.2 µm and 0.6 ± 0.1 µm, respectively; Fig. 1d–i). To examine cell-wall texture and microfibril orientation, we used field emission scanning electron microscopy (FESEM) on cryo-planed sections of *Calliarthron* genicula. We imaged the outermost wall layer of genicular cells, which consist of the earliest deposited primary walls (Fig. 1f), and the innermost wall layer representing the most recently deposited secondary walls (Fig. 1i). Fiber-like structures were observed at both the outer surface and the innermost wall layer of genicular cells but both lacked any predominant alignment (Fig. 1f, i).

Using carbohydrate-binding modules (CBMs) specific to crystalline cellulose (CBM3a) and amorphous cellulose (CBM28), putative differences in crystalline and amorphous cellulose deposition were found in primary and secondary walls of *Calliarthron* (Fig. 2a,b). Both types of cellulose were detected in primary and secondary walls and middle lamella (Fig. 2a, b), but crystalline cellulose was localized mostly to secondary walls and amorphous cellulose was localized mostly to primary walls (Fig. 2c).

Stretched genicular tissue exhibited a J-shaped stress–strain curve with an extended yield to break (Fig. 3a). Genicular tissue was remarkably extensible with a breaking strain of 103.4 ± 8.2%, which was largely unchanged with the addition of secondary walls (119.6 ± 9.4%, $P = 0.17$, Fig. 4a, b). Even with secondary walls, genicula were 3–5 times more extensible than other seaweed tissues and 10–100 times more extensible than vascular plant tissues (Fig. 3b). Genicular tissue became 20% stronger with the addition of secondary walls, from 21.5 ± 1.1 to 25.1 ± 1.5 MPa ($P < 0.05$, Fig. 3a, b). Genicular strength was intermediate between seaweed and vascular plant tissues: with secondary walls, genicula were approximately 10 times stronger than tissues from other seaweeds, but rarely as strong as vascular plant tissues (Fig. 3b). Genicular tissue became significantly stiffer with the addition of secondary walls, with a 54% increase in initial stiffness (i.e., initial slope of stress–strain curve or "Young's modulus") from 17.9 ± 2.3 to 27.6 ± 3.1 MPa ($P < 0.01$, Fig. 3a, b). Final stiffness was always greater than initial stiffness, but it was generally unchanged during the deposition of secondary walls, from 42.9 ± 3.7 to 46.1 ± 5.6 MPa ($P > 0.05$, Fig. 3a). The addition of secondary walls significantly increased the toughness of genicular tissue (i.e., area under the stress–strain curve) by 67% from 10.9 ± 1.2 to 18.2 ± 2.1 MJ/m^3 ($P < 0.01$, Fig. 3a, b). With secondary walls, genicula were up to 180 times tougher than other seaweeds and vascular plants (Fig. 3b).

Discussion

Despite ostensible similarities of secondary walls produced by land plants and coralline red algae, data presented here suggest that significant differences exist at all levels of biological organization, shedding new light on our understanding of the development and biomechanical impact of secondary cell walls in macrophytes.

The structure of secondary walls in *Calliarthron* shares similarities with both red algae and land plants. While land plants, such as *Arabidopsis*, produce very thin primary walls (less than 0.5 µm) and significantly thicker secondary walls

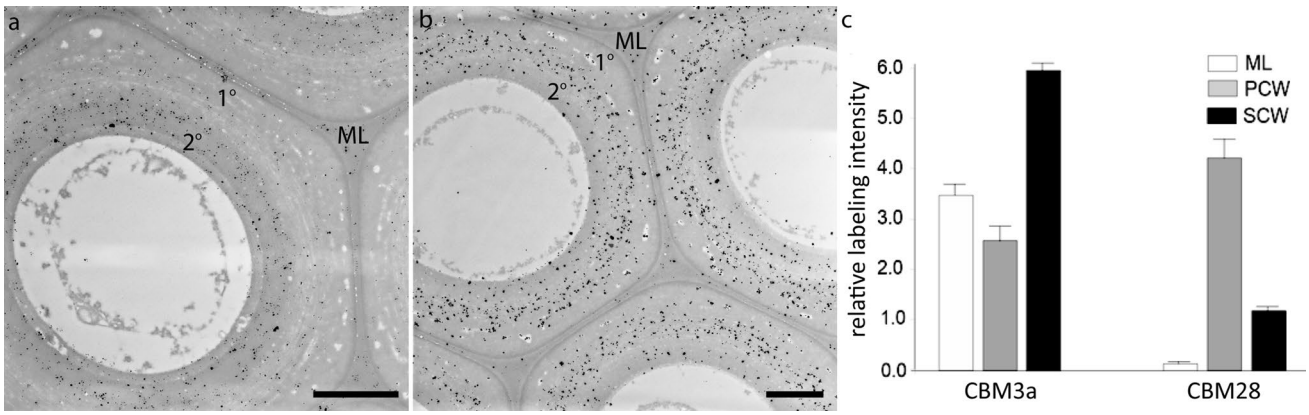

Fig. 2 Immunolabeling distinguishes crystalline and amorphous cellulose content within genicular cell walls. Crystalline cellulose and amorphous cellulose were identified using **a** CBM3a and **b** CBM28, respectively. **c** Crystalline cellulose was primarily localized in secondary cell walls (SCW) of genicula, with less localization in primary cell walls (PCW) and middle lamella (ML); amorphous cellulose was primarily localized in primary cell wall. Scale bars 1 µm (**a**, **b**)

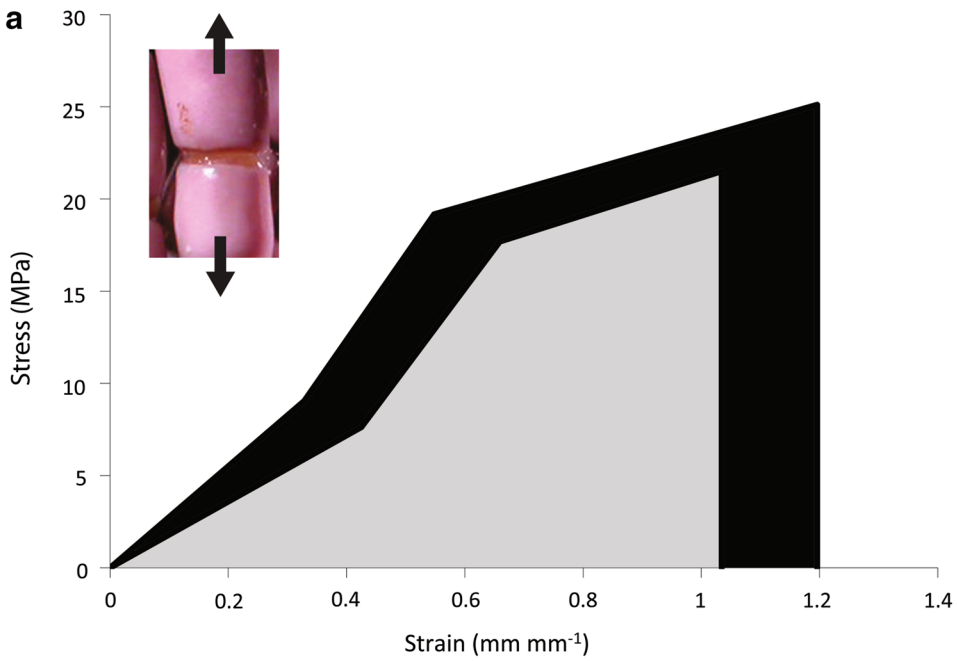

b

	Extensibility (%)	Strength (MPa)	Stiffness (MPa)	Toughness (MJ m^{-3})	Reference
***Calliarthron* geniculum**					
1° wall only	103.4 ± 8.2	21.5 ± 1.1	17.9 ± 2.3	10.9 ± 1.2	*This study*
1° + 2° walls	119.6 ± 9.4	25.1 ± 1.5	27.6 ± 3.1	18.2 ± 2.1	*This study*
Fleshy macroalgae					
Red (N = 7)	14 - 79	0.2 - 8.1	0.16 - 48.7	0.08 - 0.67	Hale 2001
Brown (N = 10)	11 - 33	1.0 - 5.1	4.5 - 40.6	0.1 - 1.1	Hale 2001
Green (N = 3)	15 - 39	0.2 - 0.9	0.64 - 4.98	0.05 - 0.13	Hale 2001
Angiosperms, seagrasses					
Phyllospadix sp.	5	12.8	152	0.29	Hale 2001
Zostera marina	6	2	46.7	0.06	Patterson et al. 2001
Angiosperms, terrestrial					
Arabidopsis stem	3	10.2	450	15.3	Kohler and Spatz 2002
Bamboo fiber	1	503	3591	3.5	Rao and Rao 2007
Banana fiber	3	600	1785	10.1	Rao and Rao 2007
Coconut fiber	20	500	250	50.0	Rao and Rao 2007
Date fiber	3	309	1132	4.2	Rao and Rao 2007
Yew wood	1	120	-	0.5	Gordon 1978

Fig. 3 Biomechanical properties of *Calliarthron* geniculum, including a comparison with other plant and algal tissues. **a** Representative stress–strain curves of immature geniculum (with only primary wall) and mature geniculum (with primary and secondary walls). Initial stiffness (E_{init}), final stiffness (E_{final}), transition strain ($\varepsilon_{transition}$), yield strain (ε_{yield}), and breaking strain (ε_{break}) are indicated. Toughness of immature and mature geniculum is represented by gray shading and black shading, respectively. **b** Summary of mechanical properties of *Calliarthron* geniculum, fleshy macroalgae, seagrasses, and land plants

(S1: 0.1–0.3 µm; S2: 1–10 µm; S3: 0.5–1.10 µm; Plomion et al. 2001), primary and secondary walls in *Calliarthron* species are nearly identical in thickness. Moreover, if primary walls in *Calliarthron* thalli are approximately 8% cellulose and the addition of secondary walls increases cellulose content up to 15%, then we estimate the cellulose content of secondary walls alone to be approximately 22%. Cellulose content in *Calliarthron* thalli is higher than most red and brown macroalgae (1–8%; Kloareg and Quatrano 1988), similar to that of *Arabidopsis* primary walls (10–20%; Carroll et al. 2012), but only half that of *Arabidopsis* secondary walls (40%; Carroll et al. 2012). Thus, while the level of wall thickening and cellulosic enrichment is far less than that in land plants, the addition of secondary walls in *Calliarthron* species appears to be an effective way to increase cellulose content beyond what is typical in marine macroalgae.

Contrary to our hypothesis that genicular cells have well-ordered cellulose microfibrils, due to their distinctive secondary walls and the anisotropic nature of their cell shape and mechanical properties, microfibrils in *Calliarthron* do not exhibit predominant orientations. Instead, genicular cell walls appear structurally similar to other red algal cell walls (Tsekos et al. 1993) in lacking the highly organized, parallel arrangement of microfibrils observed in the secondary walls of *Arabidopsis* and woody plants (Koyama et al. 1997; Nishiyama 2009; De Micco et al. 2010). Despite their lack

of parallel organization, *Calliarthron* microfibrils are similar in appearance to those observed in land plants and in other Florideophyte red algae (Tsekos et al. 1993).

Primary and secondary cell walls in *Calliarthron* geniculа differ not only in cellulose content, but also in cellulose organization, with crystalline cellulose and amorphous cellulose partly co-localizing in primary and secondary walls but crystalline cellulose being more abundant in secondary walls. Such observations suggest that several factors may influence the crystallization and assembly of cellulose during synthesis and patterning of genicular cell wall microstructure, including the differential expression of genes involved in cellulose synthesis, the xylogalactan matrix environment, and the forces exerted during wall development. The identification of cellulose microfibrils in the genicular middle lamella is surprising but may be partially explained by the poorly defined distinction between middle lamella and primary wall. During early genicular cell development, we speculate that cellulose may be displaced to the cell wall periphery to be left in close proximity to the intercellular boundary and perhaps even associate with $CaCO_3$ crystals that initially calcify and fuse adjacent walls prior to decalcification (Johansen 1981; Martone et al. 2010).

The addition of secondary walls has a significant—although relatively minor—effect on the biomechanical properties of *Calliarthron* genicular tissues. Stretched genicular tissue, both with and without secondary walls, exhibit a J-shaped stress–strain curve similar to other red algal tissues (Hale 2001), but with an extended yield to break. That is, even with the addition of secondary walls, stretched genicula more than double in length before breaking—an astounding feat that distinguishes these tissues from other algal and plant tissues. Given the remarkable extensibility of genicula, we speculate that cellulose chains are likely to be relatively short or have increased crystallinity that would limit their interactions with the xylogalactan matrix (Martone et al. 2010; Janot 2018), consistent with the microfibril length regulation model (Wasteneys 2004) and recent biomechanical models (Denny and King 2016). Contrary to the pattern observed in land plants, the addition of secondary walls only slightly increases the stiffness of genicular tissue, which generally remains quite flexible. Ongoing research suggests that abrupt increases in genicular stiffness at approximately 30–40% strain may reflect, first, the re-orientation and alignment of disorganized cellulose microfibrils and, second, the failure and slippage of newly aligned microfibrils through the cell wall matrix (Denny and King 2016; Janot 2018), but this remains to be proven. The addition of secondary walls does, however, increase the strength of genicular walls by approximately 20% and nearly doubles the toughness—both of which likely stem from the extra cell-wall material, comprising 30–50% of genicular cross sections (Martone 2007a), and the additional cellulose deposited within secondary walls. Thus, secondary walls in *Calliarthron* species fortify genicula against wave-induced breakage without sacrificing extensibility—a very different strategy than that utilized by woody plants, which strengthen, stiffen, and become inextensible with age. Interestingly, by accounting for the quantity of cell wall in cross-sections, previous work concluded that thickened wall material was similar in stiffness but not as strong as primary wall alone, suggesting that the addition of secondary walls may perhaps compensate for weakening primary wall material (Martone 2007a). The distinctive mechanical properties of corallinoid genicula, which are intermediate between macroalgae and land plants, continue to present an exciting avenue for further research.

In conclusion, secondary cell walls in *Calliarthron* have almost three-times more cellulose (~ 22% w/w) than primary walls (~ 8% w/w), as secondary wall deposition doubles wall thickness and increases total cellulose content up to 15% w/w. Cellulose bundles appear to be cylindrical and highly disorganized throughout both primary and secondary walls, with crystalline cellulose localized mostly within secondary walls. The addition of secondary walls alters some—but not all—of the biomechanical properties of *Calliarthron* genicula. With secondary walls, genicula become significantly stronger and tougher; however, despite their thickened walls, mature genicula remain uniquely extensible, more than doubling in length before breaking in tension. Thus, unlike in land plants, secondary walls help *Calliarthron* genicula resist breakage yet remain flexible as they permit fronds to go-with-the-flow along wave-battered coastlines throughout the NE Pacific.

Author contribution statement PTM and JME conceived of the study. PTM conducted biomechanical experiments and analyzed those data with KJ. MF generated electron micrographs and analyzed those data with GW. KR and JPJ performed immunolabeling experiments and analyzed those data together. JME extracted cell wall constituents and analyzed chemical data. PTM wrote the manuscript with substantive input from all authors.

Acknowledgements We would like to thank Chris Somerville and Mark Denny for all of their support and insight during the early development of this project. We thank the UBC BioImaging Facility for state-of-the-art infrastructure and technical assistance. We thank Paul Knox (Leeds, UK) and H. Gilbert (Newcastle) for providing CBM3a and CBM28 to K. R. and J-P. J. This manuscript benefitted from helpful discussions with Mark Denny, Shawn Mansfield, and Sam Starko. P. T. M. acknowledges support from a Natural Sciences and Engineering Research Council (NSERC) Discovery Grant, and J. M. E to ANPCyT (PICT2016-0132 and PICT2017-0066) and ICGEB (CRP/ARG16-03).

References

Arioli T, Peng L, Betzner AS et al (1998) Molecular analysis of cellulose biosynthesis in *Arabidopsis*. Science 279:717–720

Bilan MI, Usov AI (2001) Polysaccharides of calcareous algae and their effect on the calcification process. Russ J Bioorg Chem 27:2–16

Blake AW, McCartney L, Flint JE et al (2006) Understanding the biological rationale for the diversity of cellulose-directed carbohydrate-binding modules in prokaryotic enzymes. J Biol Chem 281:29321–29329. https://doi.org/10.1074/jbc.M605903200

Burgert I (2006) Exploring the micromechanical design of plant cell walls. Am J Bot 93:1391–1401. https://doi.org/10.3732/ajb.93.10.1391

Carroll A, Mansoori N, Li S et al (2012) Complexes with mixed primary and secondary cellulose synthases are functional in Arabidopsis plants. Plant Physiol 160:726–737. https://doi.org/10.1104/pp.112.199208

Cases MR, Stortz CA, Cerezo AS (1994) Structure of the 'corallinans'—sulfated xylogalactans from *Corallina officinalis*. Int J Biol Macromol 16:93–97. https://doi.org/10.1016/0141-8130(94)90021-3

Chantreau M, Chabbert B, Billiard S et al (2015) Functional analyses of cellulose synthase genes in flax (*Linum usitatissimum*) by virus-induced gene silencing. Plant Biotechnol J 13:1312–1324. https://doi.org/10.1111/pbi.12350

Cosgrove DJ (2005) Growth of the plant cell wall. Nat Rev Mol Cell Biol 6:850–861. https://doi.org/10.1038/nrm1746

Cosgrove DJ, Jarvis MC (2012) Comparative structure and biomechanics of plant primary and secondary cell walls. Front Plant Sci 3:204. https://doi.org/10.3389/fpls.2012.00204

De Micco V, Ruel K, Joseleau J-P, Aronne G (2010) Building and degradation of secondary cell walls: are there common patterns of lamellar assembly of cellulose microfibrils and cell wall delamination? Planta 232:621–627. https://doi.org/10.1007/s00425-010-1202-1

Delmer DP (1991) The biochemistry of cellulose synthesis. In: Lloyd CW (ed) The cytoskeletal basis of plant growth and form. Academic Press, London, pp 100–107

Denny MW, King FA (2016) The extraordinary joint material of an articulated coralline alga. II. Modeling the structural basis of its mechanical properties. J Exp Biol 219:1843–1850. https://doi.org/10.1242/jeb.138867

Denny M, Mach K, Tepler S, Martone P (2013) Indefatigable: an erect coralline alga is highly resistant to fatigue. J Exp Biol 216:3772–3780. https://doi.org/10.1242/jeb.091264

Dodgson KS, Price RG (1962) A note on the determination of the ester sulphate content of sulphated polysaccharides. Biochem J 84:106–110

Dubois M, Gilles KA, Hamilton JK et al (1956) Calorimetric method of determination of sugars and related substances. Anal Chem 28:350–356

Emons AMC, Schel JHN, Mulder BM (2002) The geometrical model for microfibril deposition and the influence of the cell wall matrix. Plant Biol 4:22–26. https://doi.org/10.1055/s-2002-20432

Evert RF (2006) Esau's plant anatomy: meristems, cells, and tissues of the plant body: their structure, function, and development, 3rd edn. Wiley-Interscience, Hoboken

Foissner I, Wasteneys GO (2012) The characean internodal cell as a model system for studying wound healing. J Microsc 247:10–22. https://doi.org/10.1111/j.1365-2818.2011.03572.x

Foissner I, Wasteneys GO (2014) Characean internodal cells as a model system for the study of cell organization. In: Jeon KW (ed) International review of cell and molecular biology. Academic Press, Burlington, pp 307–364

Fujita M, Wasteneys GO (2014) A survey of cellulose microfibril patterns in dividing, expanding, and differentiating cells of *Arabidopsis thaliana*. Protoplasma 251:687–698. https://doi.org/10.1007/s00709-013-0571-2

Gabrielson PW, Miller KA, Martone PT (2011) Morphometric and molecular analyses confirm two distinct species of *Calliarthron* (Corallinales, Rhodophyta), a genus endemic to the northeast Pacific. Phycologia 50:298–316. https://doi.org/10.2216/10-42.1

Geitmann A (2010) Mechanical modeling and structural analysis of the primary plant cell wall. Curr Opin Plant Biol 13:693–699. https://doi.org/10.1016/j.pbi.2010.09.017

Giddings TH, Brower DL, Staehelin LA (1980) Visualization of particle complexes in the plasma membrane of *Micrasterias denticulata* associated with the formation of cellulose fibrils in primary and secondary cell walls. J Cell Biol 84:327–339. https://doi.org/10.1083/jcb.84.2.327

Gierlinger N (2014) Revealing changes in molecular composition of plant cell walls on the micron-level by Raman mapping and vertex component analysis (VCA). Front Plant Sci 5:306. https://doi.org/10.3389/fpls.2014.00306

Gordon JE (1978) Structures: or why things don't fall down. Penguin Books, Harmondsworth

Hale B (2001) Macroalgal materials: foiling fracture and fatigue from fluid forces. Stanford University, PhD

Harris PJ (2006) Primary and secondary plant cell walls: a comparative overview. N Zeal J For Sci 36:36–53

Heaney-Kieras J, Roden L, Chapman DJ (1977) The covalent linkage of protein to carbohydrate in the extracellular protein-polysaccharide from the red alga *Porphyridium cruentum*. Biochem J 165:1–9

Janot K (2018) Mechanical and chemical convergence of joints in three lineages of articulated coralline algae. Ph.D. thesis, University of British Columbia, Canada

Janot K, Martone PT (2016) Convergence of joint mechanics in independently evolving, articulated coralline algae. J Exp Biol 219:383–391. https://doi.org/10.1242/jeb.131755

Johansen HW (1981) Coralline algae, a first synthesis. CRC Press Inc., Boca Raton

Joseleau J-P, Perez S (2016) The plant cell walls. http://www.glycopedia.eu/IMG/pdf/theplantcellwalls.pdf. Accessed 4 Mar 2019

Kim N-H, Herth W, Vuong R, Chanzy H (1996) The cellulose system in the cell wall of *Micrasterias*. J Struct Biol 117:195–203. https://doi.org/10.1006/jsbi.1996.0083

Kloareg B, Quatrano RS (1988) Structure of the cell wall of marine algae and ecophysiological functions of the matrix polysaccharides. Ocean Mar Biol Ann Rev 26:259–315

Köhler L, Spatz H-C (2002) Micromechanics of plant tissues beyond the linear-elastic range. Planta 215:33–40. https://doi.org/10.1007/s00425-001-0718-9

Kolender AA, Matulewicz MC, Cerezo AS (1995) Structural analysis of antiviral sulfated alpha-D-(1→3)-linked mannans. Carbohydr Res 273(2):179–185

Koyama M, Helbert W, Imai T et al (1997) Parallel-up structure evidences the molecular directionality during biosynthesis of bacterial cellulose. Proc Natl Acad Sci USA 94:9091–9095

Lehtiö J, Sugiyama J, Gustavsson M et al (2003) The binding specificity and affinity determinants of family 1 and family 3 cellulose binding modules. Proc Natl Acad Sci USA 100:484–489. https://doi.org/10.1073/pnas.212651999

Li S, Bashline L, Lei L, Gu Y (2014) Cellulose synthesis and its regulation. The arabidopsis book, 2014(12). https://doi.org/10.1199/tab.0169

Marga F, Grandbois M, Cosgrove DJ, Baskin TI (2005) Cell wall extension results in the coordinate separation of parallel microfibrils: evidence from scanning electron microscopy and atomic force microscopy. Plant J 43:181–190. https://doi.org/10.1111/j.1365-313X.2005.02447.x

Martone PT (2006) Size, strength and allometry of joints in the articulated coralline *Calliarthron*. J Exp Biol 209:1678–1689
Martone PT (2007a) Kelp versus coralline: cellular basis for mechanical strength in the wave-swept seaweed *Calliarthron* (Corallinaceae, Rhodophyta). J Phycol 43:882–891
Martone PT (2007b) Biomechanics of flexible joints in the calcified seaweed *Calliarthron cheilosporioides*. Ph.D. thesis, Stanford University
Martone PT, Denny MW (2008) To break a coralline: mechanical constraints on the size and survival of a wave-swept seaweed. J Exp Biol 211:3433–3441
Martone PT, Estevez JM, Lu FC et al (2009) Discovery of lignin in seaweed reveals convergent evolution of cell-wall architecture. Curr Biol 19:169–175
Martone PT, Navarro DA, Stortz CA, Estevez JM (2010) Differences in polysaccharide structure between calcified and uncalcified segments in the coralline *Calliarthron cheilosporioides* (Corallinales, Rhodophyta). J Phycol 46:507–515. https://doi.org/10.1111/j.1529-8817.2010.00828.x
Matulewicz MC, Cerezo AS, Jarret RM, Syn N (1992) High resolution 13C-n.m.r. spectroscopy of 'mixed linkage' xylans. Int J Biol Macromol 14:29–32
Mayhew TM, Griffiths G, Lucocq JM (2004) Applications of an efficient method for comparing immunogold labelling patterns in the same sets of compartments in different groups of cells. Histochem Cell Biol 122:171–177. https://doi.org/10.1007/s00418-004-0685-x
McLean BW, Boraston AB, Brouwer D et al (2002) Carbohydrate-binding modules recognize fine substructures of cellulose. J Biol Chem 277:50245–50254. https://doi.org/10.1074/jbc.M204433200
Morrison IM (1988) Hydrolysis of plant cell walls with trifluoroacetic acid. Phytochemistry 27:1097–1100
Morrison JC, Greve LC, Richmond PA (1993) Cell wall synthesis during growth and maturation of *Nitella* internodal cells. Planta 189:321–328. https://doi.org/10.1007/BF00194428
Mutwil M, Debolt S, Persson S (2008) Cellulose synthesis: a complex complex. Curr Opin Plant Biol 11:252–257. https://doi.org/10.1016/j.pbi.2008.03.007
Myers A, Preston RD (1959) Fine structure in the red algae. III. A general survey of cell-wall structure in the red algae. Proc R Soc Lond Ser B Biol Sci. https://doi.org/10.1098/rspb.1959.0034
Navarro DA, Stortz CA (2002) Isolation of xylogalactans from the Corallinales: influence of the extraction method on yields and compositions. Carbohydr Polym 49:57–62
Niklas KJ (2004) The cell walls that bind the tree of life. BioScience 54:831. https://doi.org/10.1641/0006-3568(2004)054%5b0831:tcwtbt%5d2.0.co;2
Nishiyama Y (2009) Structure and properties of the cellulose microfibril. J Wood Sci 55:241–249. https://doi.org/10.1007/s10086-009-1029-1
Patterson MR, Harwell MC, Orth LM, Orth RJ (2001) Biomechanical properties of the reproductive shoots of eelgrass. Aquat Bot 69:27–40
Plomion C, Leprovost G, Stokes A (2001) Wood formation in trees. Plant Physiol 127:1513. https://doi.org/10.1104/pp.010816
Rao KMM, Rao KM (2007) Extraction and tensile properties of natural fibers: *Vakka*, date and bamboo. Compos Struct 77:288–295. https://doi.org/10.1016/j.compstruct.2005.07.023
Ruel K, Chabannes M, Boudet A-M et al (2001) Reassessment of qualitative changes in lignification of transgenic tobacco plants and their impact on cell wall assembly. Phytochemistry 57:875–882. https://doi.org/10.1016/S0031-9422(01)00118-2
Ruel K, Nishiyama Y, Joseleau J-P (2012) Crystalline and amorphous cellulose in the secondary walls of *Arabidopsis*. Plant Sci 193–194:48–61. https://doi.org/10.1016/j.plantsci.2012.05.008
Rydahl MG, Fangel JU, Mikkelsen MD et al (2015) *Penium margaritaceum* as a model organism for cell wall analysis of expanding plant cells. Methods Mol Biol 1242:1–21. https://doi.org/10.1007/978-1-4939-1902-4_1
Salmén L (2015) Wood morphology and properties from molecular perspectives. Ann For Sci 72:679–684. https://doi.org/10.1007/s13595-014-0403-3
Salmén L, Burgert I (2009) Cell wall features with regard to mechanical performance. A review COST action E35 2004–2008: wood machining—micromechanics and fracture. Holzforschung. https://doi.org/10.1515/hf.2009.011
Saxena IM, Brown RM (2005) Cellulose biosynthesis: current views and evolving concepts. Ann Bot 96:9–21. https://doi.org/10.1093/aob/mci155
Sethaphong L, Haigler CH, Kubicki JD et al (2013) Tertiary model of a plant cellulose synthase. Proc Natl Acad Sci USA 110:7512–7517. https://doi.org/10.1073/pnas.1301027110
Somerville C (2006) Cellulose synthesis in higher plants. Annu Rev Cell Dev Biol 22:53–78. https://doi.org/10.1146/annurev.cellbio.22.022206.160206
Somerville C, Bauer S, Brininstool G et al (2004) Toward a systems approach to understanding plant cell walls. Science 306:2206–2211. https://doi.org/10.1126/science.1102765
Stevenson TT, Furneaux RH (1991) Chemical methods for the analysis of sulphated galactans from red algae. Carbohydr Res 210:277–298
Stortz CA, Cerezo AS (2000) Novel findings in carrageenans, agaroids and "hybrids"red seaweed galactans. Curr Top Phytochem 4:121–134
Sugimoto K, Williamson RE, Wasteneys GO (2000) New techniques enable comparative analysis of microtubule orientation, wall texture, and growth rate in intact roots of Arabidopsis. Plant Physiol 124:1493–1506
Takano R, Hayashi J, Hayashi K, Hara S, Hirase S (1996) Structure of a water-soluble polysaccharide sulfate from the red seaweed *Joculator maximus* Manza. Bot Mar 39:95–102
Thomas LH, Forsyth VT, Sturcova A et al (2013) Structure of cellulose microfibrils in primary cell walls from collenchyma. Plant Physiol 161:465–476. https://doi.org/10.1104/pp.112.206359
Tsekos I (1999) The sites of cellulose synthesis in algae: diversity and evolution of cellulose-synthesizing enzyme complexes. J Phycol 35:635–655. https://doi.org/10.1046/j.1529-8817.1999.3540635.x
Tsekos I, Reiss HD, Schnepf E (1993) Cell-wall structure and supramolecular organization of the plasma membrane of marine red algae visualized by freeze fracture. Acta Botanica Neerlandica 42:119–132
Turner SR, Somerville CR (1997) Collapsed xylem phenotype of *Arabidopsis* identifies mutants deficient in cellulose deposition in the secondary cell wall. Plant Cell 9:689–701
Usov AI, Bilan MI (1996) Polysaccharides from algae. 49. Isolation of alginic acid, sulfated xylogalactan and floridean starch from calcareous red alga *Bossiella cretacea* (P. et R.) Johansen (Rhodophyta, Corallinaceae). Bioorg Khim 22:126–133
Usov AI, Bilan MI, Shashkov AS (1997) Structure of a sulfated xylogalactan from the calcareous red alga *Corallina pilulifera* P. et R. (Rhodophyta, Corallinaceae). Carbohydr Res 303:93–102
Voiniciuc C, Pauly M, Usadel B (2018) Monitoring polysaccharide dynamics in the plant cell wall. Plant Physiol 176:2590–2600. https://doi.org/10.1104/pp.17.01776
Waaland SD, Waaland JR (1975) Analysis of cell elongation in red algae by fluorescent labelling. Planta 126:127–138
Wasteneys GO (2004) Progress in understanding the role of microtubules in plant cells. Curr Opin Plant Biol 7:651–660
Yamaguchi M, Mitsuda N, Ohtani M et al (2011) VASCULAR-RELATED NAC-DOMAIN 7 directly regulates the expression

of a broad range of genes for xylem vessel formation. Plant J 66:579–590. https://doi.org/10.1111/j.1365-313X.2011.04514.x

Yoon HS, Hackett JD, Ciniglia C et al (2004) A molecular timeline for the origin of photosynthetic eukaryotes. Mol Biol Evol 21:809–818